Negative Band Gaps in Dilute InN_xSb_{1-x} Alloys

T. D. Veal, I. Mahboob, and C. F. McConville*

Department of Physics, University of Warwick, Coventry CV4 7AL, United Kingdom

(Received 21 July 2003; published 1 April 2004)

A thin layer of InNSb has been fabricated by low energy nitrogen implantation in the near-surface region of InSb. X-ray photoelectron spectroscopy indicates that nitrogen occupies ~6% of the anion lattice sites. High-resolution electron-energy-loss spectroscopy of the conduction band electron plasma reveals the absence of a depletion layer for this alloy, thus indicating that the Fermi level is located below the valence band maximum (VBM). The plasma frequency for this alloy combined with the semiconductor statistics indicates that the Fermi level is located above the conduction band minimum (CBM). Consequently, the CBM is located *below* the VBM, indicating a negative band gap material has been formed. These measurements are consistent with $\mathbf{k}\cdot\mathbf{p}$ calculations for $InN_{0.06}Sb_{0.94}$ that predict a semimetallic band structure.

DOI: 10.1103/PhysRevLett.92.136801 PACS numbers: 73.20.Mf, 71.20.Nr, 71.55.Eq, 73.61.Ey

Alloying semiconductors with large size-mismatched atoms induces unusual electronic properties that can be exploited in a range of otherwise unavailable applications, such as long wavelength lasers and high performance solar cells. In III-V semiconductors, the replacement of a few per cent of the group V element by small, highly electronegative and isoelectronic nitrogen atoms results in a dramatic reduction of the fundamental band gap of approximately 100 meV per atomic per cent of nitrogen [1,2]. This enables the band gap of the resulting dilute III-V nitride alloys to be tuned to particular energies for optoelectronic applications by changing the nitrogen content. Since only small amounts of nitrogen are required to produce large changes in the band gap, the alloy can be almost lattice matched to existing substrate material, enabling high quality alloys to be grown epitaxially and incorporated into the existing optoelectronics infrastructure.

From a fundamental point of view, several researchers have considered the possibility of both band gap closure and "negative" band gaps in these dilute III-N-V semiconductors. Theoretical investigations have concentrated on GaN_xAs_{1-x} alloys with relatively large x values [3–6]. In one study, the possibility of negative band gaps was discounted for ordered GaN_xAs_{1-x} alloys on the basis of quasiparticle calculations with a many-body correction [7]. In fact, since the theoretical calculations are mostly for ordered alloys which have greater band gap bowing than the random alloys produced by epitaxial growth, band gap closure is even less likely to be found experimentally in GaN_xAs_{1-x} [5]. Experimental studies have shown that GaN_xAs_{1-x} is a direct gap semiconductor for $x \leq 14.8\%$ [8]. Extending the experimental search for band gap closure by growing GaN_xAs_{1-x} alloys with larger x values is complicated by several factors, such as the lattice mismatch of greater than 20% between GaAs and GaN [5]. Additionally, the phase stability of GaN_xAs_{1-x} alloys must be considered [3]. If a miscibility gap exists, the realization of a negative band gap alloy may be prohibited by the solid solution of GaN_xAs_{1-x} being thermodynamically unstable at the appropriate x values. Indeed, a negative band gap has not previously been realized in any III-N-V alloy.

An alternative approach to observing band gap closure and negative band gaps in III-N-V materials is to incorporate nitrogen in a narrow gap III-V semiconductor; a semimetallic material has been predicted to result from the giant band gap bowing that occurs when relatively low percentages of anion sites of InSb are occupied by nitrogen [9]. Since the band gap of InSb (180 meV at 300 K) is approximately one-eighth of that of GaAs, band gap closure in InN_xSb_{1-x} is predicted to occur at much lower x values than in GaN_xAs_{1-x}.

In order to predict the variation of the band gap as a function of nitrogen incorporation in InSb, the band structure of InN_xSb_{1-x} has been calculated using a modified $\mathbf{k}\cdot\mathbf{p}$ Hamiltonian originally developed for GaN_xAs_{1-x} and successfully applied to InN_xSb_{1-x} [10–12]. Modified $\mathbf{k}\cdot\mathbf{p}$ calculations of band gaps have been shown, by comparison with tight binding calculations, to be accurate up to nitrogen concentrations corresponding to $x = 0.1$ [13]. The $\mathbf{k}\cdot\mathbf{p}$ approximation, which models the interactions between the conduction band and the valence bands, is modified to include the interaction of a localized N level with the conduction band of the InSb host. The nitrogen level, E_{N_0}, is located at 740 meV above the InSb valence band maximum [14]. The decrease in the energy of the effective nitrogen level as x increases is described by $E_N = E_{N_0} - \gamma x$, where $\gamma = 2.47$ eV [14]. This variation of the effective nitrogen level is a result of interactions between neighboring resonances [13]. The conduction and valence band edges and nitrogen level as a function of nitrogen content, calculated using the modified $\mathbf{k}\cdot\mathbf{p}$ Hamiltonian, are shown in Fig. 1. The interaction of the extended Γ states of the conduction band of the host semiconductor with the localized

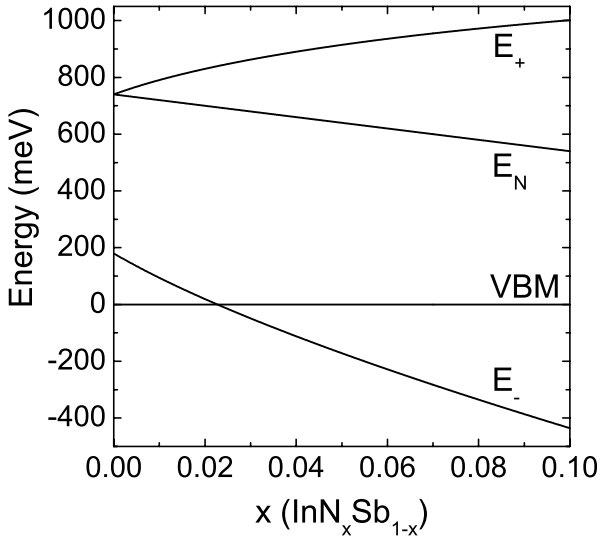

FIG. 1. The conduction and valence band edges and nitrogen level of InN_xSb_{1-x} at 300 K as a function of x, calculated using a modified $\mathbf{k} \cdot \mathbf{p}$ Hamiltonian with the nitrogen level (at $x = 0$) at 740 meV above the valence band maximum.

N-induced resonant states results in the formation of two nonparabolic subbands, E_+ and E_-. The band gap reaches zero at $x \sim 0.022$ and at higher x values the band gap is negative; the E_- conduction band minimum (CBM) is below the valence band maximum (VBM), indicating that the alloy is semimetallic.

In this Letter, we present experimental evidence of a negative band gap in InN_xSb_{1-x} alloys created by nitrogen implantation into InSb. Since optical experimental techniques are of limited use for characterizing extremely narrow gap semiconductors and semimetals because of the Moss-Burstein shift, the nitrided InSb has been investigated by high-resolution electron-energy-loss spectroscopy (HREELS).

The samples used were from a bulk grown wafer of InSb(111)*A* (Ge doped, $p \sim 1 \times 10^{15}$ cm^{-3}). These InSb surfaces were prepared *in situ* by 45 min of 2 keV N_2^+ ion bombardment at normal incidence using a sample current of 4 mA, giving a total ion dose of 4×10^{16} cm^{-2}. This was followed by a 60 min radiative anneal at 550 K. X-ray photoelectron spectroscopy (XPS) of the In 3*d*, Sb 3*d*, and N 1*s* core level spectra was performed using a Scienta ESCA300 spectrometer, employing a high-power (3.5 kW) rotating anode and monochromated Al-K_α source ($h\nu = 1486.6$ eV), high transmission electron optics, and a multichannel electron detector. Emissions angles of 90° and 30° were used to vary the effective photoelectron escape depth to assess the uniformity of the bombarded layer in the near-surface region. The HREELS experiments were performed using a specular scattering geometry with an incident and scattered polar angle of 45°.

An XPS spectrum of the N 1*s* region, recorded at normal emission after N_2 ion bombardment and annealing (IBA) of the InSb(111)*A*, is shown in Fig. 2. Deconvolution of the spectrum was achieved by peak fitting using a Shirley background and a series of Voigt functions. There are three contributions to the N 1*s* spectrum: substitutional N bonded to In at a binding energy of 396.9 eV, N bonded to both In and Sb (In-N-Sb) at 397.9 eV [15,16], and N-Sb at 399.0 eV [17,18]. The N bonded to In contributes $(72 \pm 3)\%$ of the total N 1*s* signal at both emission angles. The composition of the nitrided layer has been determined from the areas of the In 3*d*, Sb 3*d*, and N 1*s* core level spectra, taking account of the different atomic sensitivity factors. Since only N substituted on group V sites contributes to the characteristic band structure modification of dilute III-V nitrides, only the N-In component of the N 1*s* spectrum was included. The compositions determined from XPS spectra recorded using normal emission are 50.5% In, 46.5% Sb, and 3.0% N, and, at grazing emission are 53.2% In, 43.9% Sb, and 2.9% N. These translate into an approximate alloy composition of $InN_{0.06}Sb_{0.94}$. The proportion of N does not change significantly with emission angle, suggesting that the alloy composition is approximately uniform over the depth of ~60 Å probed by the XPS. The slight increase in the relative amount of In at the more grazing emission angle is because, as indicated by low energy electron diffraction, the InSb(111)*A* surface exhibited an In-rich (2×2) reconstruction after N_2 IBA.

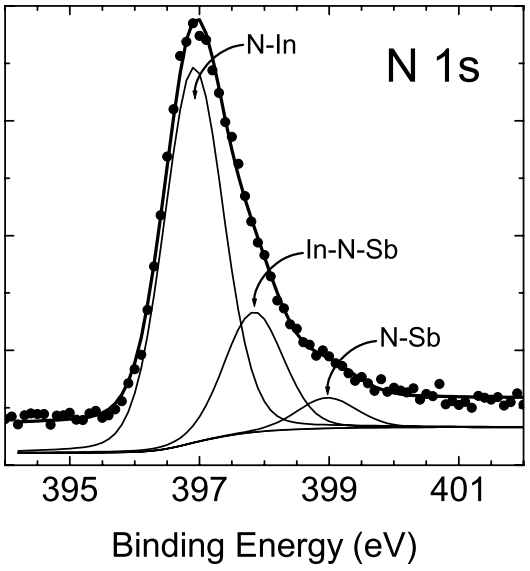

FIG. 2. An XPS spectrum of the N 1*s* region (dots) recorded using normal emission from InSb(111)*A* after N_2 ion bombardment and annealing. The deconvolution of the spectra into the different chemically shifted components (vertically offset thin lines) and the sum of these contributions (thick line) are also shown.

Using HREELS to study conduction band electron plasmon excitations, the variation of the electronic properties with depth can be probed by changing the kinetic energy of the impinging electrons so that different parallel wave vectors are excited, altering the effective maximum probing depth in the range 100–1000 Å. A series of normalized HREEL spectra, recorded with a range of incident electron energies (E_i) from the nitrided InSb, is shown in Fig. 3, along with dielectric theory simulations. The shoulder on the loss energy side of the elastic peak, which increases in intensity as E_i is reduced, is due to Fuchs-Kliewer surface phonon excitations at 23 meV. The other feature of the spectra is the plasmon peak centered at 59 meV at 5 eV and the 20 meV downward dispersion it undergoes as a function of increasing E_i [Fig. 3(b)]. This can be explained in terms of the existence of a region close to the surface of higher plasma frequency than in the bulk. As the incident electron energy is increased, the effective probing depth increases and so the higher plasma frequency layer contributes proportionally less to the electron-energy-loss spectrum.

This explanation is quantitatively confirmed by semiclassical dielectric theory simulations of the HREEL spectra. A layered model of the sample is used to approximate the smooth variation of the plasma frequency with depth. We have applied this approach previously to successfully describe the dielectric response in the near-surface region of narrow gap III-V semiconductors [19,20]. Briefly, simulations are generated using a local dielectric function for each one of several uniform layers. The layer dielectric functions each contain a background term, a phonon term, and a plasma term based on the hydrodynamic model. A five-layer model was employed, consisting of a 20 Å plasma-free "dead" layer (to represent the quantum mechanical decline of the electron wave functions to zero at the surface), a second 150 Å thick layer with a plasma frequency of 65 meV, two further layers with plasma frequencies of 47 and 32 meV, and a semi-infinite bulk layer with a plasma frequency of 12 meV. This layered structure of the near-surface region was used to reproduce the variation of the phonon and plasmon peak energy and intensity with probing electron energy. The first and second layers used in the HREELS simulations are associated with the $InN_{0.06}Sb_{0.94}$ alloy detected by XPS. The other layers represent the region from the $InN_{0.06}Sb_{0.94}$ layer to the bulk InSb.

The band structure of the $InN_{0.06}Sb_{0.94}$ near-surface layer has been calculated and indicates that the E_- CBM is 240 meV *below* the VBM as shown in Fig. 4. The E_- conduction band dispersion relation has been used to calculate the carrier statistics of this layer, including the plasma frequency and the effective mass at the Fermi level as a function of carrier concentration [12]. The plasma frequency of 65 meV in the $InN_{0.06}Sb_{0.94}$ layer corresponds to a free electron density, n, of 1.6×10^{18} cm^{-3} and a Fermi level of 140 meV *above* the CBM (Fig. 4). Donorlike defects, such as the Sb vacancy, created by the implantation process, contribute to the enhanced plasma frequency and raise the Fermi level in the near-surface region with respect to the CBM.

A depletion layer of greater than 60 Å (depending on the bulk doping level) normally exists at the surface of InSb as a result of Fermi level pinning by occupied negatively charged acceptor-type surface states, N_A^-, that lie close to the effective midgap energy (the

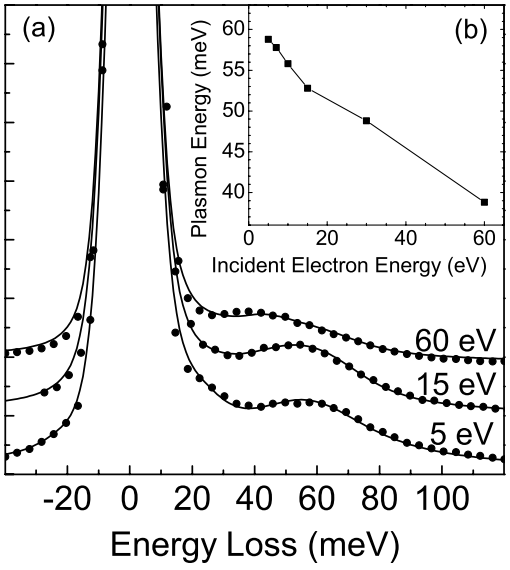

FIG. 3. (a) Probing energy-dependent experimental HREEL spectra recorded from InSb(111)A following N_2 IBA (dots), and corresponding dielectric theory simulations (solid lines). (b) The plasmon peak position as a function of the incident electron energy.

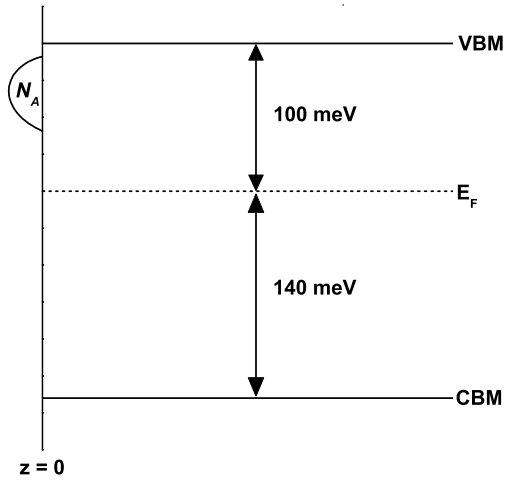

FIG. 4. The conduction band minimum (CBM) and valence band maximum (VBM) with respect to the Fermi level for $InN_{0.06}Sb_{0.94}$. Also shown at the surface ($z = 0$) are the acceptor-type surface states, N_A, located below the VBM and above E_F, making them neutral.

Γ-point VBM in InSb) [21,22]. Since the addition of nitrogen only lowers the conduction band edge in a narrow region of k space, the effective midgap energy across the entire Brillouin zone remains similar to that in InSb. Therefore, the acceptor-type surface states in InN_xSb_{1-x} still lie close to the Γ-point VBM. This observation has been confirmed with the detection of depletion layers by HREELS in InN_xSb_{1-x} alloys grown by molecular beam epitaxy with $x < 0.01$ [23]. Further, damage-induced donor defects are insufficient to explain the absence of a surface depletion layer as indicated by the HREELS results. If donor defects alone were responsible for the charge profile, a surface depletion layer would still be present, as in the case of Ar^+ ion bombarded and annealed InSb surfaces [24]. The lack of a depletion layer at the surface of the $InN_{0.06}Sb_{0.94}$ is explained by the Fermi level being *below* the acceptor-type surface states, making them unoccupied and therefore neutral. No surface depletion layer forms as there is no surface charge to be neutralized. The surface Fermi level is also known to be *above* the CBM from the aforementioned 65 meV plasma frequency and carrier statistics calculations. The VBM being *above* the Fermi level and the CBM being simultaneously *below* the Fermi level means that the VBM is *above* the CBM—the band gap in the near-surface layer is negative.

Low energy N_2 implantation into InSb at normal incidence results in the formation of a thin layer of dilute InN_xSb_{1-x} alloy. Surface chemical analysis indicates that approximately 6% of the group V lattice sites are occupied by isoelectronic nitrogen bonded to indium atoms. Calculations employing a $\mathbf{k} \cdot \mathbf{p}$ Hamiltonian to describe the interaction between the resonant nitrogen level and the InSb conduction band predict a semimetallic band structure for this alloy composition. HREELS investigations of the nitrided layer indicate that a negative band gap alloy has been formed by the nitrogen-induced shift of the conduction band. The absence of surface electron depletion indicates that the surface Fermi level is *below* the VBM and the near-surface electron plasma frequency locates the surface Fermi level *above* the CBM. These two factors can be reconciled only by the existence of a negative band gap due to the nitrogen-induced changes to the band structure, in agreement with the predictions of the $\mathbf{k} \cdot \mathbf{p}$ calculations.

We are grateful to Dr. Danny Law of the National Centre for Electron Spectroscopy and Surface (NCESS) analysis, UK, for their assistance with the XPS experiments. We also acknowledge the Engineering and Physical Sciences Research Council, UK, for financial support under Grant No. GR/R93872/01 and for access to the NCESS facility under Grant No. GR/S24252/01.

*Electronic address: C.F.McConville@warwick.ac.uk

[1] W. Shan, W. Walukiewicz, J.W. Ager, D. R. Chamberlin, E. E. Haller, J. F. Geisz, D. J. Friedman, J. M. Olson, and S. R. Kurtz, Phys. Rev. Lett. **82**, 1221 (1999).
[2] C.W. Tu, J. Phys. Condens. Matter **13**, 7169 (2001).
[3] J. Neugebauer and C. G. Van de Walle, Phys. Rev. B **51**, 10 568 (1995).
[4] L. Bellaiche, S. H. Wei, and A. Zunger, Phys. Rev. B **54**, 17 568 (1996).
[5] A. T. Lim and Y. P. Feng, Mater. Sci. Semicond. Proc. **4**, 577 (2001).
[6] B. K. Agrawal, P. S. Yadav, R. Srivastava, and S. Agrawal, J. Phys. Condens. Matter **10**, 4597 (1998).
[7] A. Rubio and M. L. Cohen, Phys. Rev. B **51**, 4343 (1995).
[8] W. G. Bi and C.W. Tu, Appl. Phys. Lett. **70**, 1608 (1997).
[9] S. Sakai, T. S. Cheng, T. C. Foxon, T. Sugahara, Y. Naoi, and H. Naoi, J. Cryst. Growth **189/190**, 471 (1998).
[10] E. P. O'Reilly and A. Lindsay, Phys. Status Solidi B **216**, 131 (1999).
[11] B. N. Murdin *et al.*, Appl. Phys. Lett. **78**, 1568 (2001).
[12] I. Mahboob, T. D. Veal, and C. F. McConville, Appl. Phys. Lett. **83**, 2169 (2003).
[13] A. Lindsay and E. P. O'Reilly, Solid State Commun. **112**, 443 (1999).
[14] A. Lindsay (private communication).
[15] J. D. Hecht, F. Frost, T. Chassé, D. Hirsch, H. Neumann, A. Schindler, and F. Bigl, Appl. Surf. Sci. **179**, 196 (2001).
[16] J. D. Hecht, F. Frost, D. Hirsch, H. Neumann, A. Schindler, A. B. Preobrajenski, and T. Chasse, J. Appl. Phys. **90**, 6066 (2001).
[17] L. Haworth, J. Lu, P. Hill, D. I. Westwood, J. E. Macdonald, N. Hartman, A. Schneider, and D. R. T. Zahn, J. Vac. Sci. Technol. B **16**, 2254 (1998).
[18] Y. Suzuki, H. Kumano, W. Tomota, N. Sanada, and Y. Fukuda, Appl. Surf. Sci. **172**, 162 (2000).
[19] Ph. Lambin, J. P. Vigneron, and A. A. Lucas, Phys. Rev. B **32**, 8203 (1985).
[20] T. D. Veal and C. F. McConville, Phys. Rev. B **64**, 085311 (2001).
[21] J. Tersoff, Phys. Rev. Lett. **52**, 465 (1984).
[22] T. S. Jones, M. O. Schweitzer, N.V. Richardson, G. R. Bell, and C. F. McConville, Phys. Rev. B **51**, 17 675 (1995).
[23] T. D. Veal, I. Mahboob, and C. F. McConville, Appl. Phys. Lett. **83**, 1776 (2003).
[24] T. S. Jones, M. Q. Ding, N.V. Richardson, and C. F. McConville, Surf. Sci. **247**, 1 (1991).